QUANTIFYING WETLAND TYPE AND ECOSYSTEM SERVICES WITH HYPERSPATIAL UAS IMAGERY

Whitney P. Broussard III

GEOG 596A
Capstone Proposal
Fall 2016

PennState

Robert P. Brooks

CRMS Wetlands
Coastwide Reference Monitoring System

JESCO ENVIRONMENTAL
& Geotechnical Services, Inc.

Tom Cousté

UNIVERSITY of LOUISIANA LAFAYETTE

Jenneke M. Visser

Louisiana is Experiencing a Coastal Crisis

Predicted Land Change over the Next 50 Years

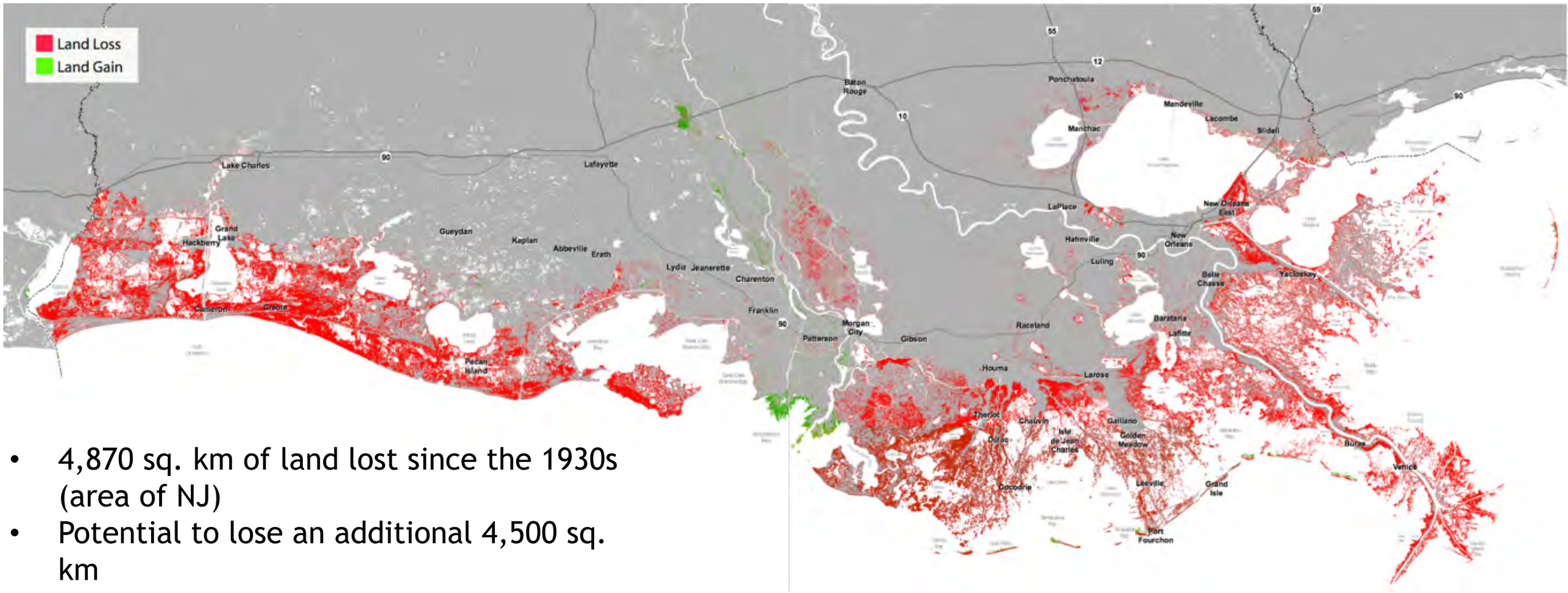

- 4,870 sq. km of land lost since the 1930s (area of NJ)
- Potential to lose an additional 4,500 sq. km

- 18% of US oil and 24% of US gas production totaling $16B USD per year
- 1st in the nation in total shipping tonnage - 20% of the nation's waterborne commerce
- $2.8B USD fisheries industry in Louisiana - 16% of US fisheries come from Louisiana coast

Louisiana's Comprehensive Master Plan for a Sustainable Coast

committed to **our coast**

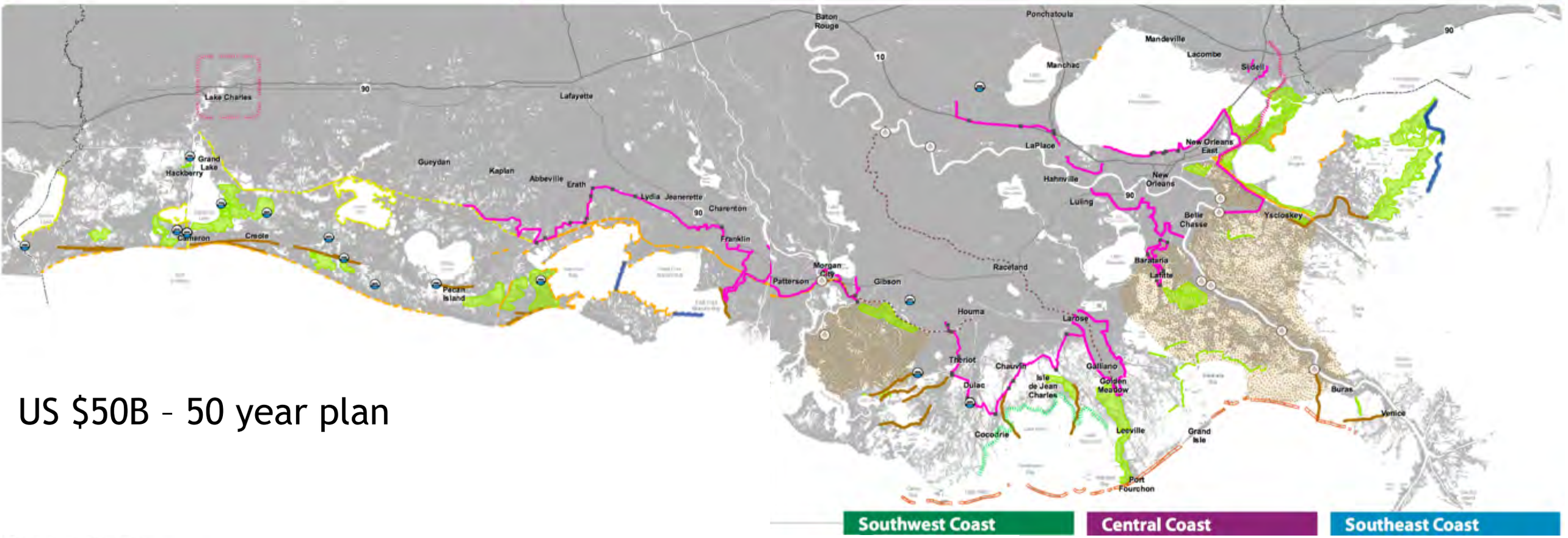

US $50B – 50 year plan

Project Types

2012 Master Plan Model Suite

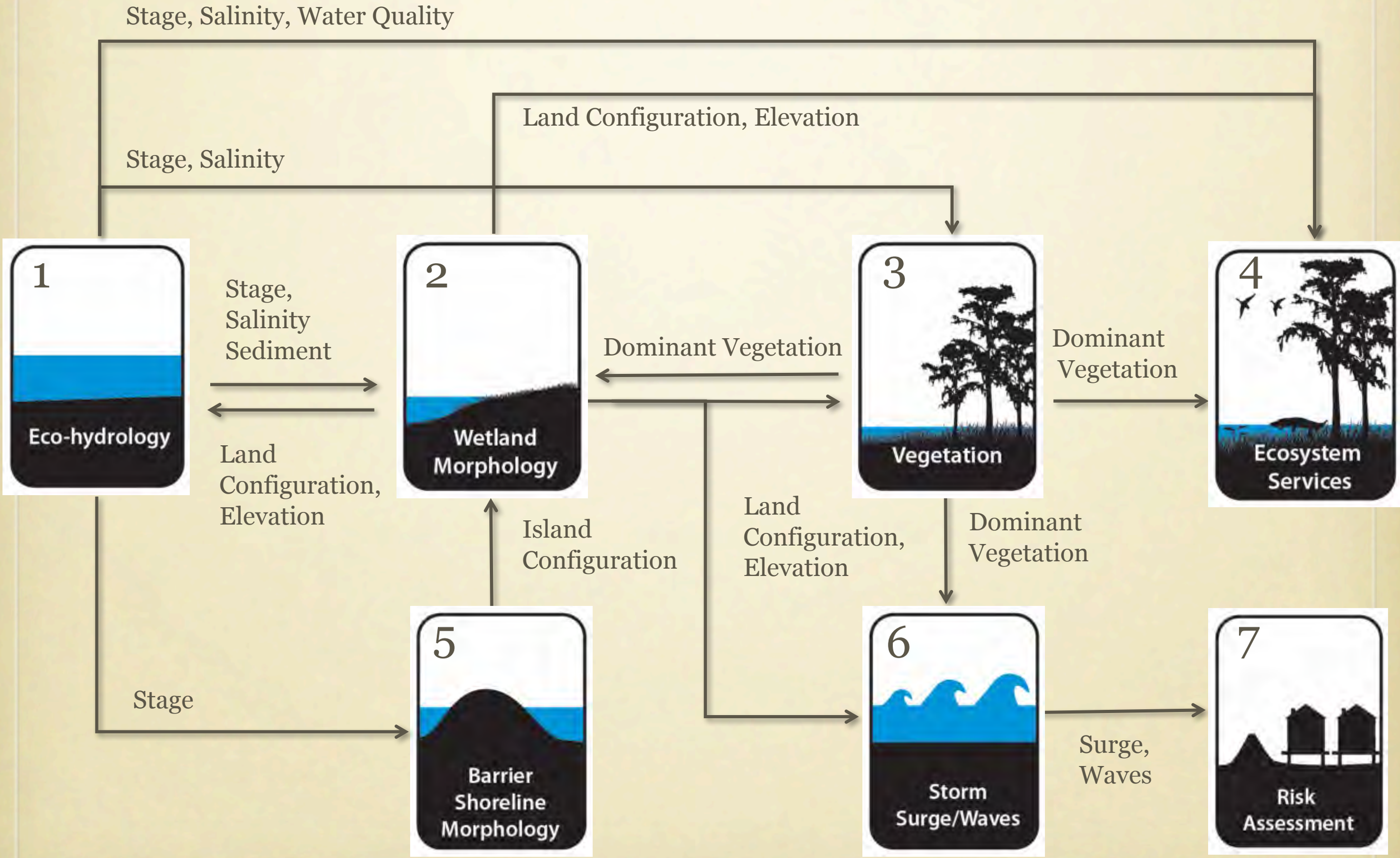

Current Wetland Vegetation Information

Coast-wide Surveys

156 North/South transects spaced 7.5 minutes apart from the Texas state line to the Mississippi state line.

Vegetative data were obtained at predetermined stations spaced 0.5 miles along each transect.

- Species identified
- Five Cover classes
  - >75%
  - 50-75%
  - 25-50%
  - 5-25%
  - <5%

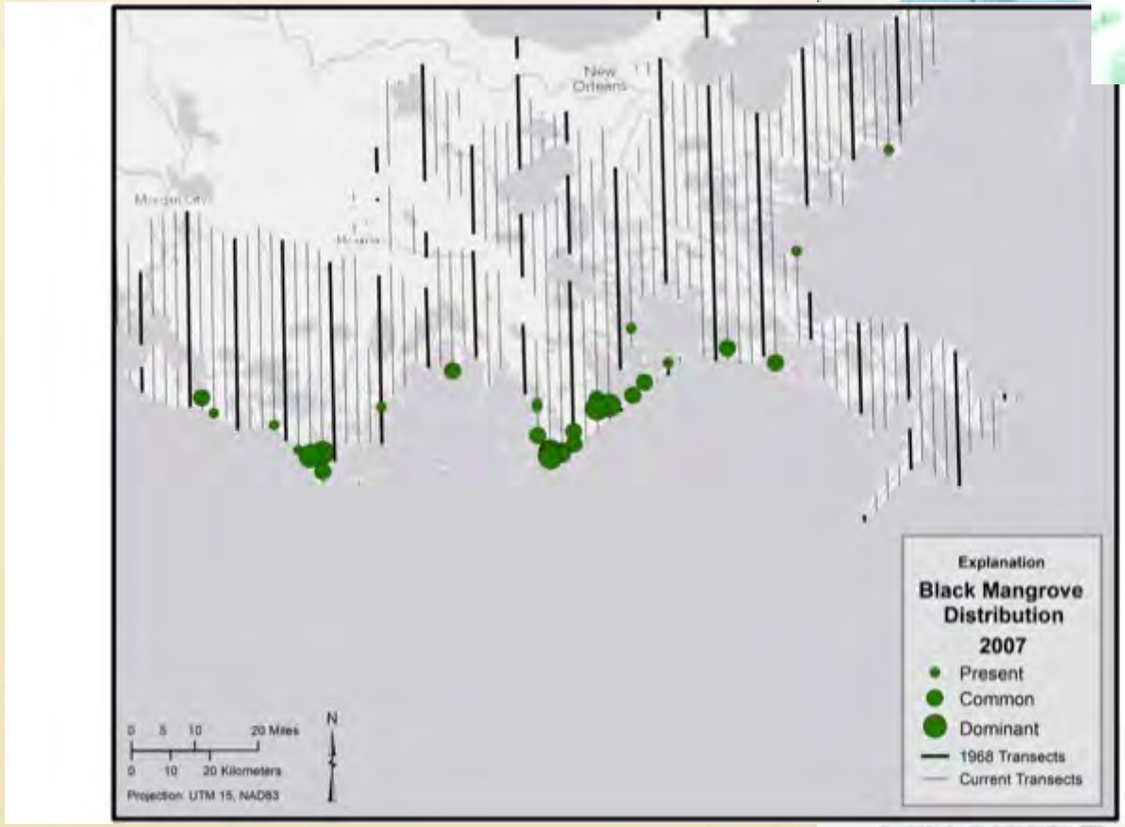

Photos: Greg Linscombe and Jenneke Visser

Coastwide Reference Monitoring System

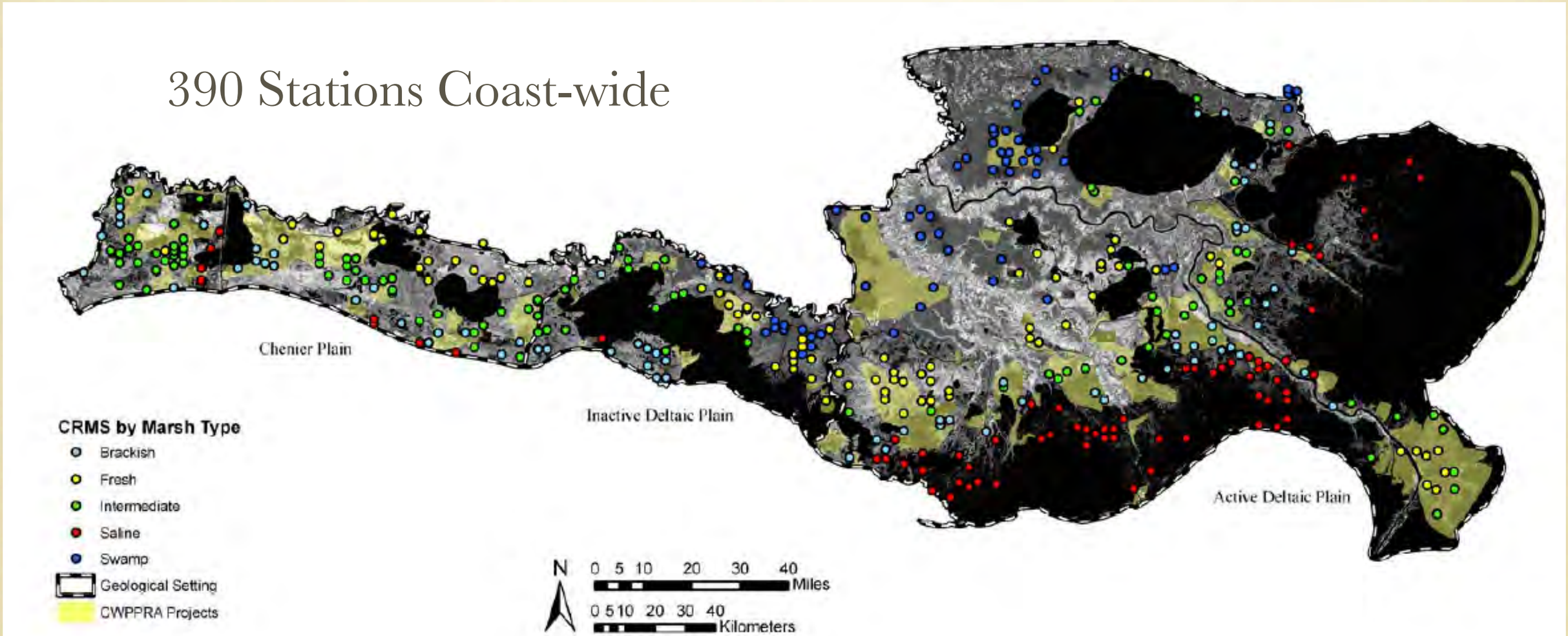

CRMS Wetlands
Coastwide Reference Monitoring System

TYPICAL CRMS SITE SAMPLING & DATA COLLECTION

Aspects of ecosystem structure and function are measured at each site including marsh elevation, vegetative assemblage, and hydrologic parameters

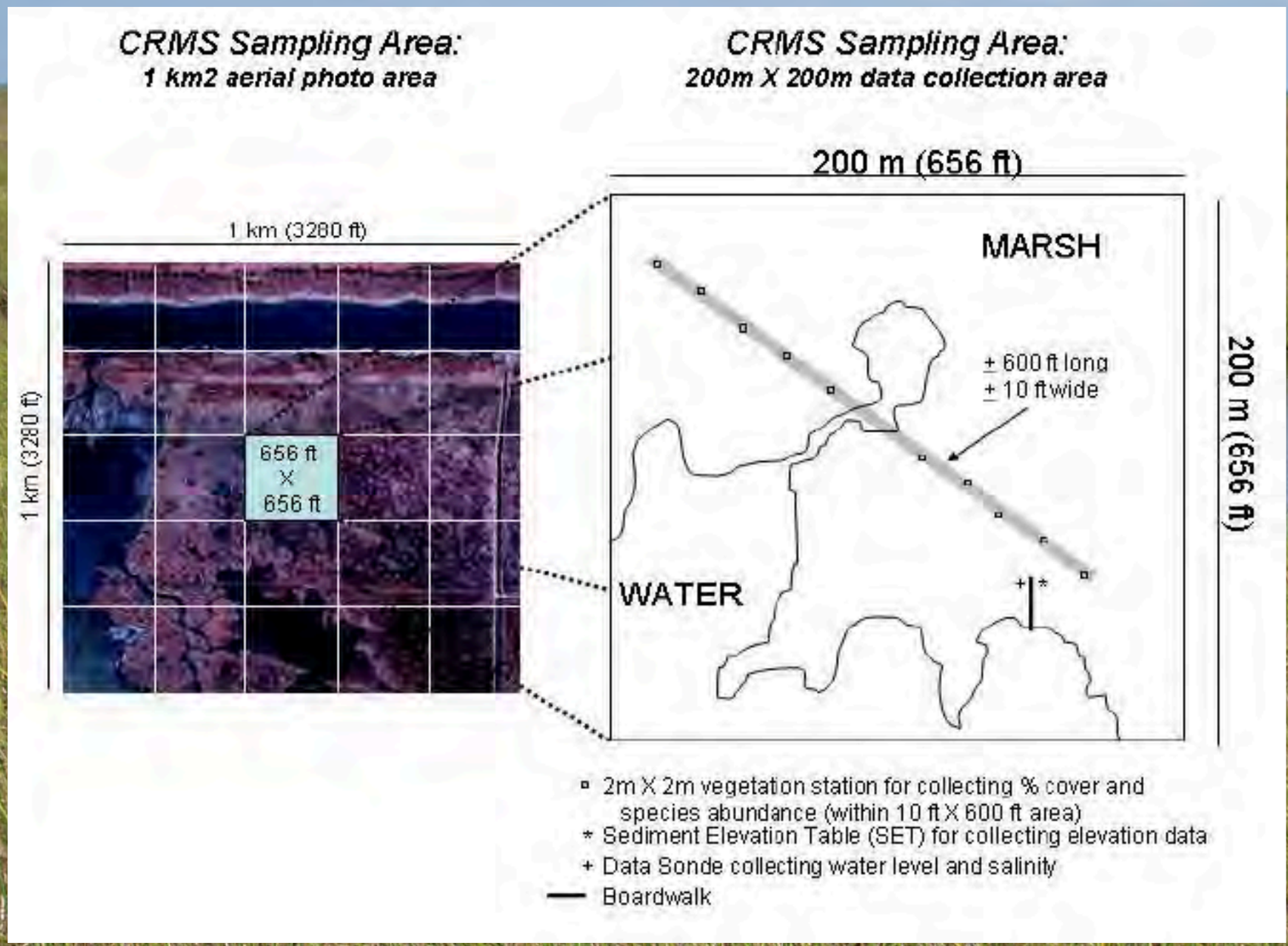

What about Unmanned Aircraft Systems (UAS)?

i. Late 1970s – first use of a fixed wing remotely controlled aircraft in photogrammetry experiments (Przybilla and Wester-Ebbinghaus 1979)
ii. 2004 - first use of a commercial low-cost model helicopter with semiautomated navigation to create a high-resolution digital terrain model (Eisenbeiss et al. 2005).
iii. Chong (2007) used high definition video to map local beach erosion.
iv. Lejot et al. (2007) used very high spatial resolution imagery to map channel bathymetry and topography.
v. **Lechner et al. (2012)** utilized hyperspatial data provided by a UAS and object-based image analysis (OBIA) methods to classify upland swamp communities.
vi. Multispectral and hyperspectral imagery used to map wetlands **(Phinn et al. 1996, Chust et al. 2008, Yang and Argtigas 2010, Klemas 2013)**.
vii. UAS are now widely used in a host of environmental applications, such as land use mapping, wetlands mapping, LIDAR bathymetry, flood and wildfire surveillance, tracking oil spills, urban studies, and Arctic ice investigations (Klemas 2015).

Comparisons between satellite data, traditional aerial photography, and UAS imagery

i. UAS technology allows flexible deployments - high-temporal and hyperspatial resolution (<1dm) data (Niethammer et al. 2012).

ii. Rocchini (2007) demonstrated that higher resolution datasets from Quickbird satellite imagery showed highly significant correlations with species richness as opposed to coarser resolution datasets from Aster and Landsat imagery, which were not highly correlated.

iii. In Coastal Louisiana, UAS have the ability to fly the current helicopter transects and to collect hyperspatial aerial images at higher frequencies. Multispecral reflectance will help automate species richness and cover estimates. Photogrammetry can provide elevation estimates and Digital Surface Models (DSM).

Landsat derived DEM – 30m GSD

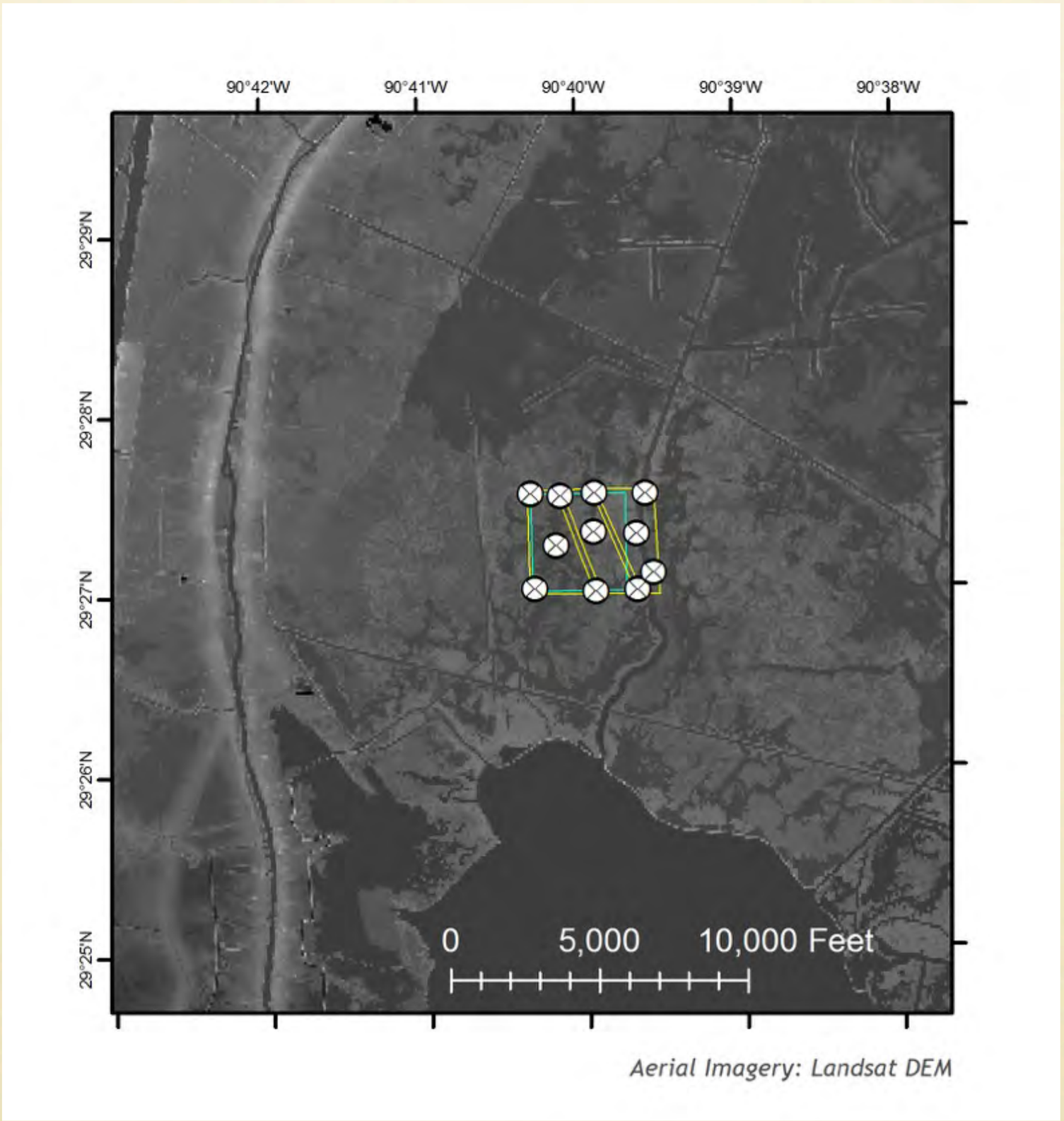

Aerial Imagery: Landsat DEM

Landsat derived DEM – 30m GSD

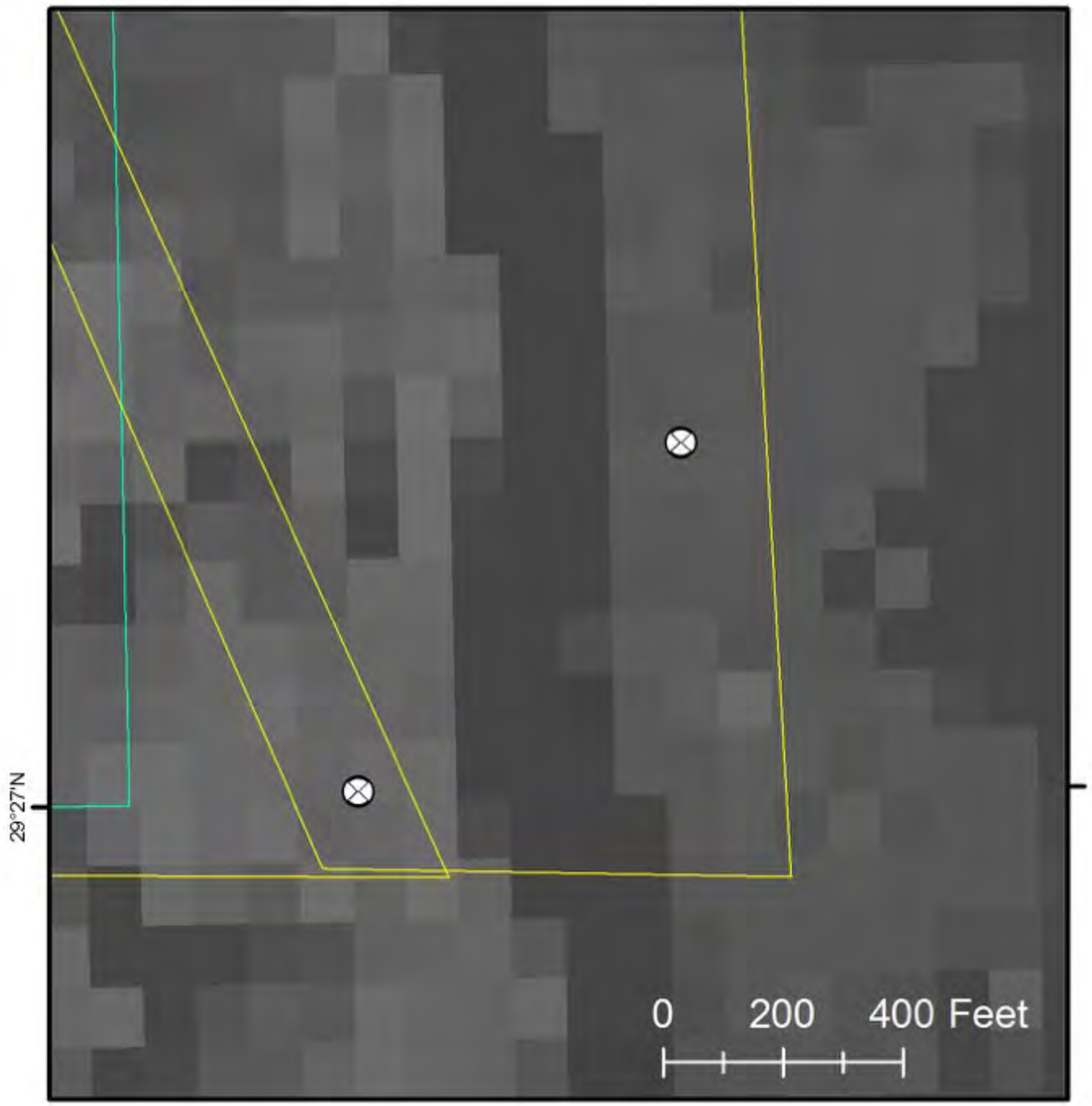

Aerial Imagery: Landsat DEM

Aerial Photography – 1m GSD

Aerial Imagery: Coastal Wetlands Planning, Protection and Restoration Act (CWPPRA), 2008

Aerial Photography – 1m GSD

Aerial Imagery: Coastal Wetlands Planning, Protection and Restoration Act (CWPPRA), 2008

UAS Aerial Photography – 2.5cm GSD

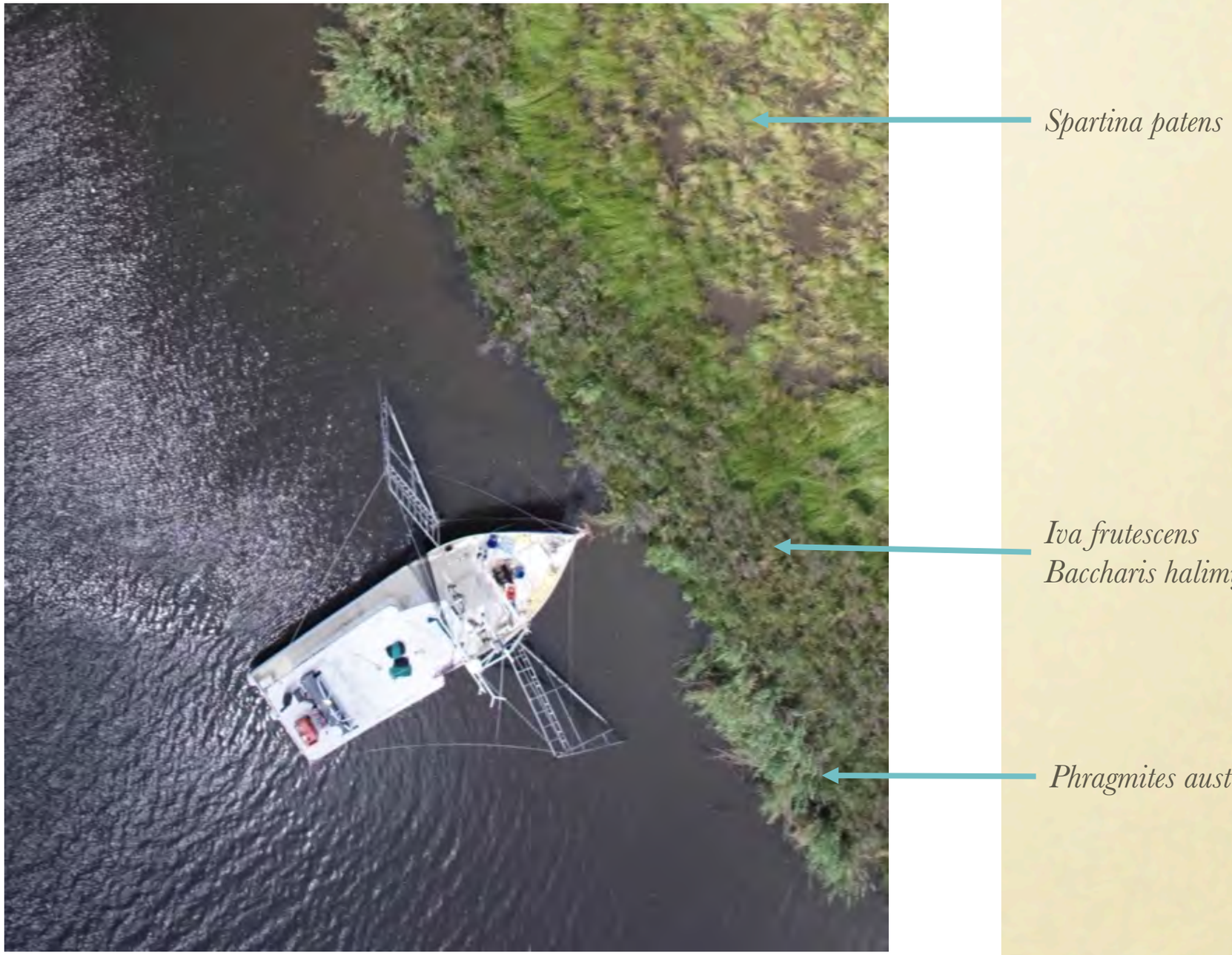

UAS Aerial Photography – 2.5cm GSD

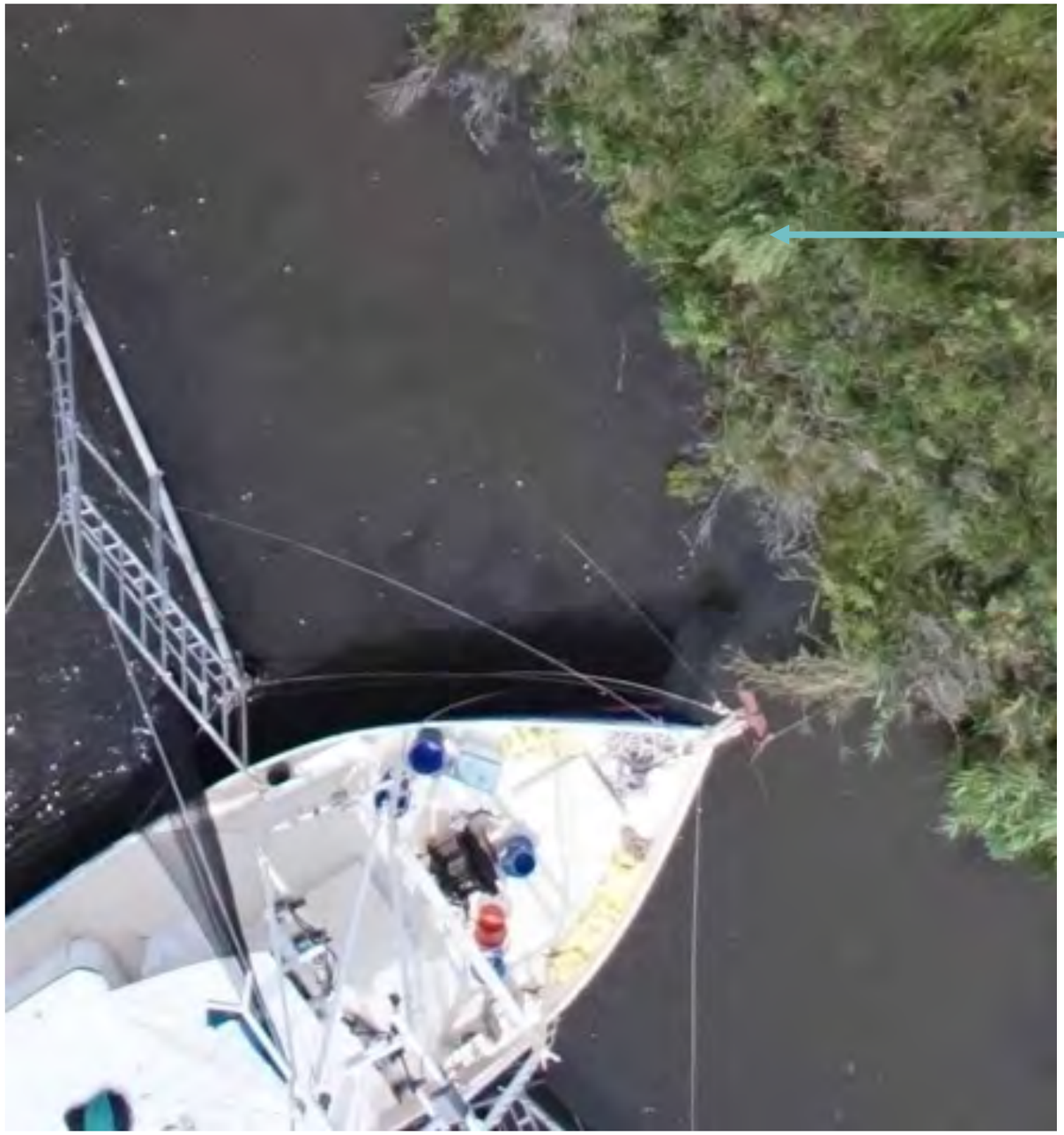

UAS Aerial Photography – 2.5cm GSD

Leaf shape/area

PROJECT GOALS AND OBJECTIVES

- This project will design a pilot study to collect hyperspatial/multispectral aerial imagery from a UAS in a brackish marsh environment in coastal Louisiana.
- The objective is to collect 2.5cm GSD RGB and NIR imagery of a 1 km^2 area.
- Create raster datasets that are georeferenced and ready for object-based image analysis

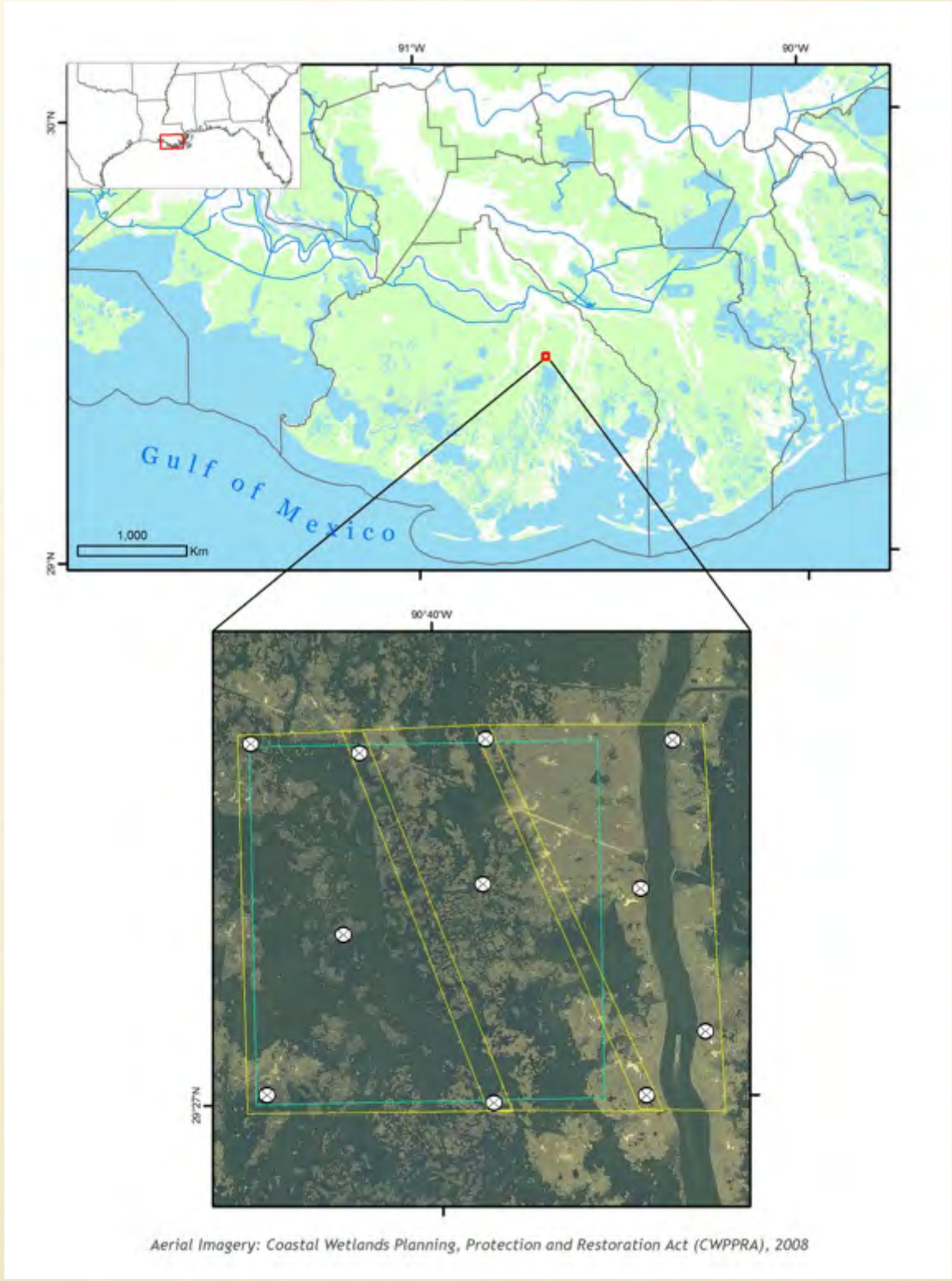

Project location in Terrebonne Parish, Louisiana. Coastwide Reference Monitoring System (CRMS) site in Cyan, Flight Blocks in yellow, GCPs are white crosses.

PROJECT GOALS AND OBJECTIVES

- Object-Based Image Analysis
  - Species composition and ecosystem service metrics
    - Land-water interface (edge habitat and fragmentation)
  - Species composition
  - Plant height
  - Aboveground biomass
  - Carbon Sequestration
  - Productivity (NDVI)

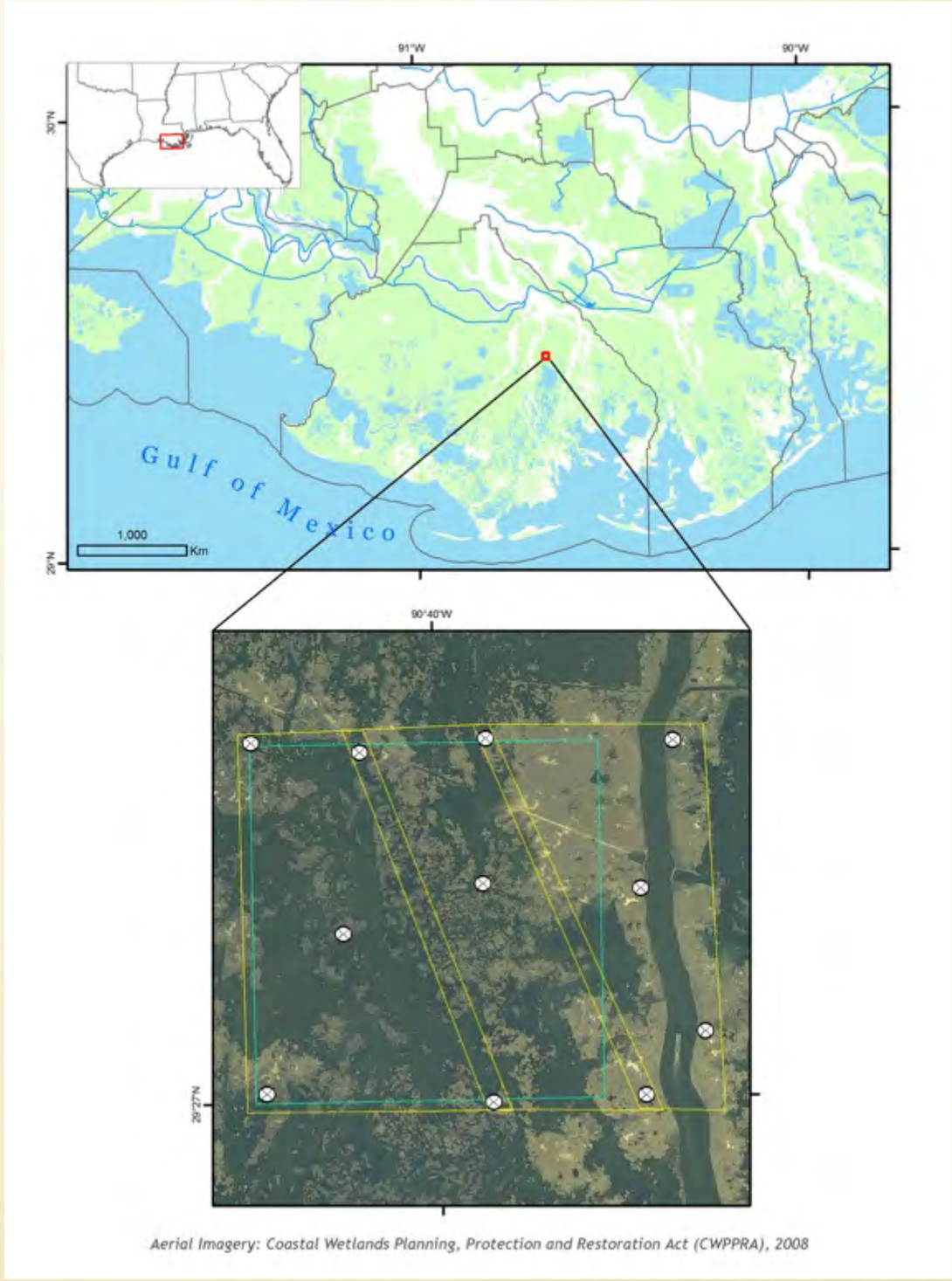

Project location in Terrebonne Parish, Louisiana. Coastwide Reference Monitoring System (CRMS) site in Cyan, Flight Blocks in yellow, GCPs are white crosses.

FIELDWORK Trimble UX5

HARDWARE

Type	Fixed wing
Weight	2.5 kg (5.51 lb)
Wingspan	1 m (3.28 ft)
Wing area	34 dm
Dimensions	100 cm x 65 cm X 10.5 cm (39.37 in x 25.59 in x 4.13 in)
Material	EPP foam; Carbon frame structure; Composite elements
Propulsion	Electric pusher propeller; brushless 700 W motor

OPERATION

Endurance[1]	50 minutes
Range[1]	60 km (37.28 mi)
Cruise speed	80 kmh (50 mph)
Maximum ceiling[2]	5000 m (16,404 ft)

ACQUISITION PERFORMANCE

Resolution (GSD)	2.0 cm to 19.5 cm (.79 in to 7.67 in)
Height above take-off location (AGL)	75 m to 750 m (246 ft to 2,460 ft)

AREA COVERAGE TABLE

Height	GSD	Coverage/flight [km^2] (1)			Coverage/day [km^2] (2)		
		70%	80%	90%	70%	80%	90%
75 m (246 ft)	2.0 cm (0.79 in)	1.1 km^2 (0.43 mi^2)	0.8 km^2 (0.31 mi^2)	0.4 km^2 (0.15 mi^2)	6.85 km^2 (2.63 mi^2)	4.5 km^2 (7.74 mi^2)	2.3 km^2 (0.88 mi^2)
100 m (328 ft)	2.6 cm (1.02 in)	1.8 km^2 (0.7 mi^2)	1.2 km^2 (0.64 mi^2)	0.6 km^2 (0.23 mi^2)	10.8 km^2 (4.17 mi^2)	7.2 km^2 (2.78 mi^2)	3.6 km^2 1.39 mi^2)
150 m (492 ft)	3.9 cm (1.54 in)	3.1 km^2 (1.2 mi^2)	2.1 km^2 (0.81 mi^2)	1.0 km^2 (0.39 mi^2)	18.7 km^2 (7.22 mi^2)	12.5 km^2 (4.83 mi^2)	6.2 km^2 (2.39 mi^2)

Sony NEX-5R camera and Voigtländer lens used in the Trimble UX5 Aerial Imaging Rover

Flight Plan

Take off and landing located north of the project area.

Sectional Aeronautical Raster Chart with project boundaries shown in red.

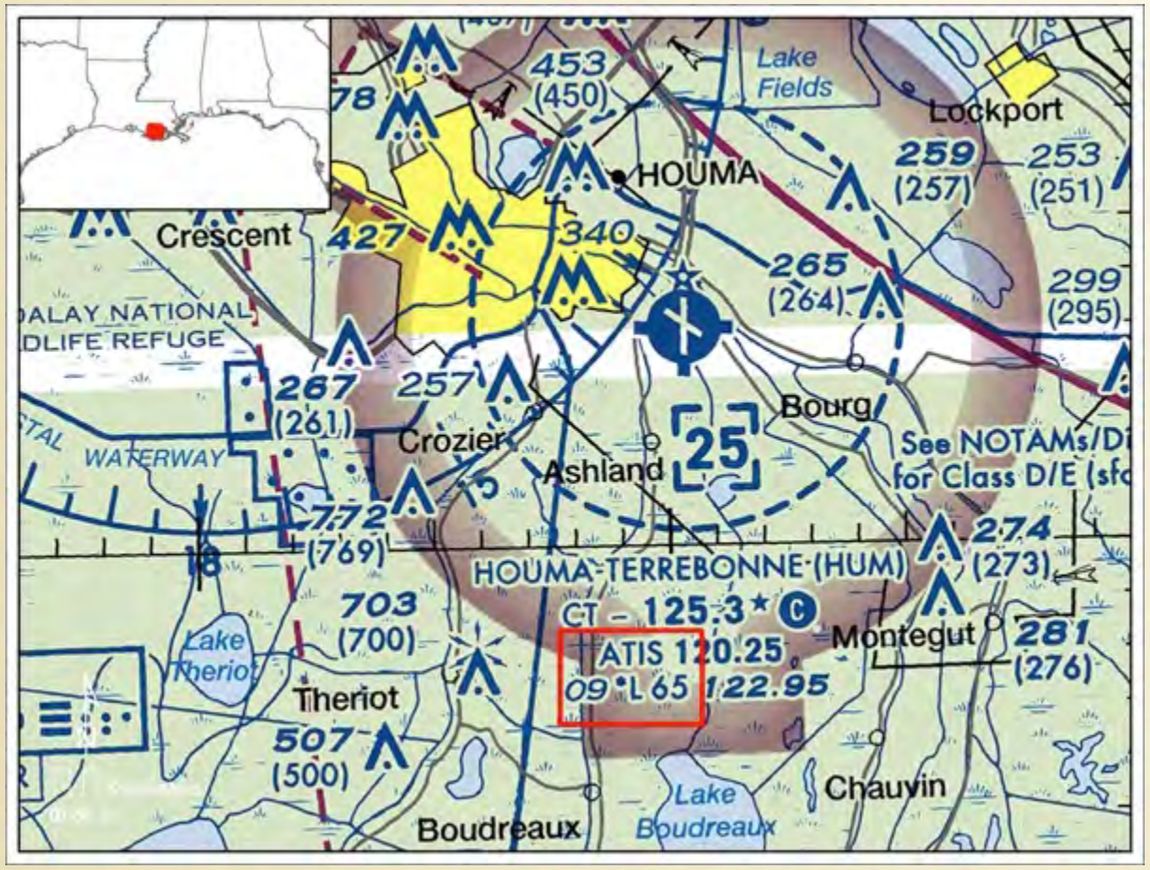

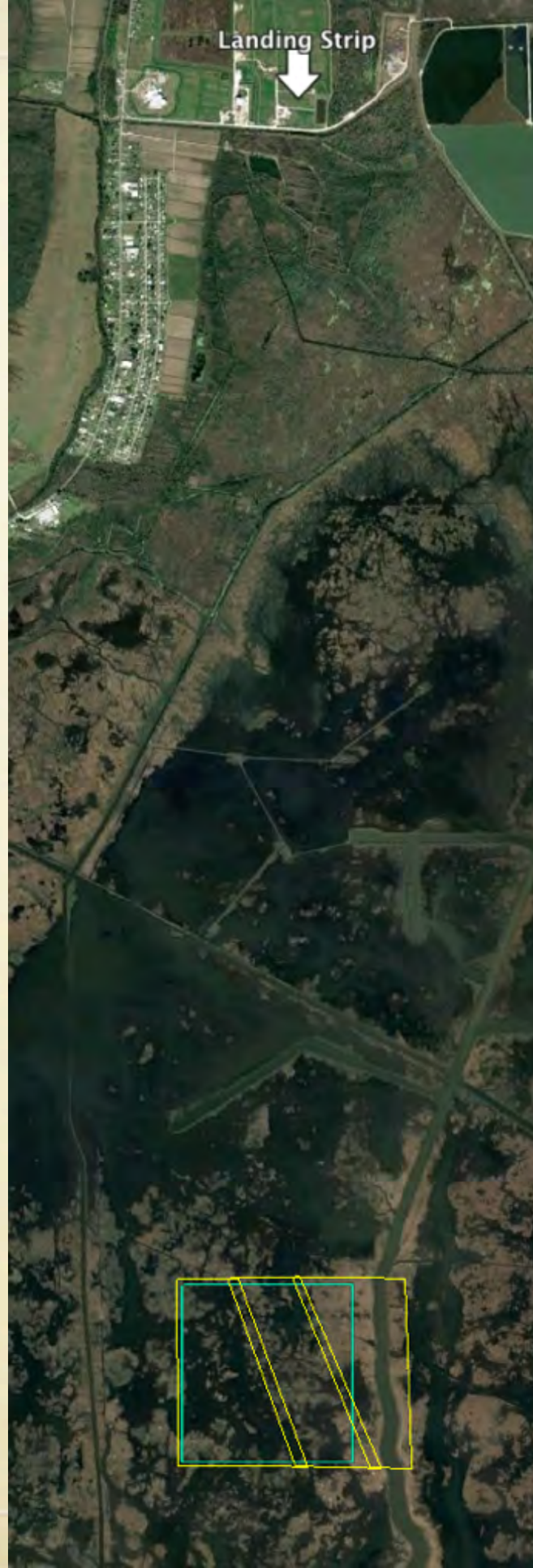

FAA Part 107 compliant operations (DO NOT UNDERESTIMATE!)

Flight Plan: Manual Calculations

Compute the Ground Coverage of Each Image

$$\begin{aligned} Ground\ Coverage &= (6000\ pixels * 1in) \times (4000\ pixels * 1in) \\ &= 6000in \times 4000in \\ &= 500ft \times 333.3ft \end{aligned}$$

Compute the Number of Flight Lines

$$\begin{aligned} Line\ Spacing\ (SP) &= Image\ coverage\ (w) * ((100 - Sidelap)/100) \\ &= 500ft * (100 - 60/100) \\ &= 200ft \end{aligned}$$

$$\begin{aligned} Number\ of\ Flight\ Lines\ (NFL) &= (Width\ of\ Project/SP) + 1 \\ &= (3{,}281ft/200ft) + 1 \\ &= 17.4 \end{aligned}$$

NFL rounds up to 18.

Flying Altitude

$$\begin{aligned} Flying\ Height\ (H) &= \frac{focal\ length\ (f) \times Ground\ Sample\ Distance\ (GSD)}{Pixel\ Width\ (ab)} \\ &= \frac{15.6mm \times 2.54cm}{3.9\mu m} \\ &= \frac{15.6mm \times 25.4mm}{0.0039mm} \\ &= 101{,}600mm \\ &= 101.6m \end{aligned}$$

Number of Images to be Acquired

$$\begin{aligned} Airbase\ (B) &= Images\ Coverage\ (H) \times ((100 - Endlap)/100) \\ &= 333.3 \times ((100 - 80)/100) \\ &= 66.6 \end{aligned}$$

$$\begin{aligned} Number\ of\ Images\ (NIM) &= (Length/B) + 1 + 4 \\ &= (3{,}281ft/66.6ft) + 1 + 4 \\ &= 54.3 \end{aligned}$$

NIM rounds up to 55.

$$\begin{aligned} Total\ Number\ of\ Images &= NFL \times NIM \\ &= 18 \times 55 \\ &= 990 \end{aligned}$$

Time Between Images

$$\begin{aligned} Time\ (t) &= Airbase\ (B)/Aircraft\ speed\ (v) \\ &= 66.6ft/80\ km\ hr^{-1} \\ &= 66.6ft/262467.2\ ft\ hr^{-1} \\ &= .000254\ hr \\ &= 0.9\ sec \end{aligned}$$

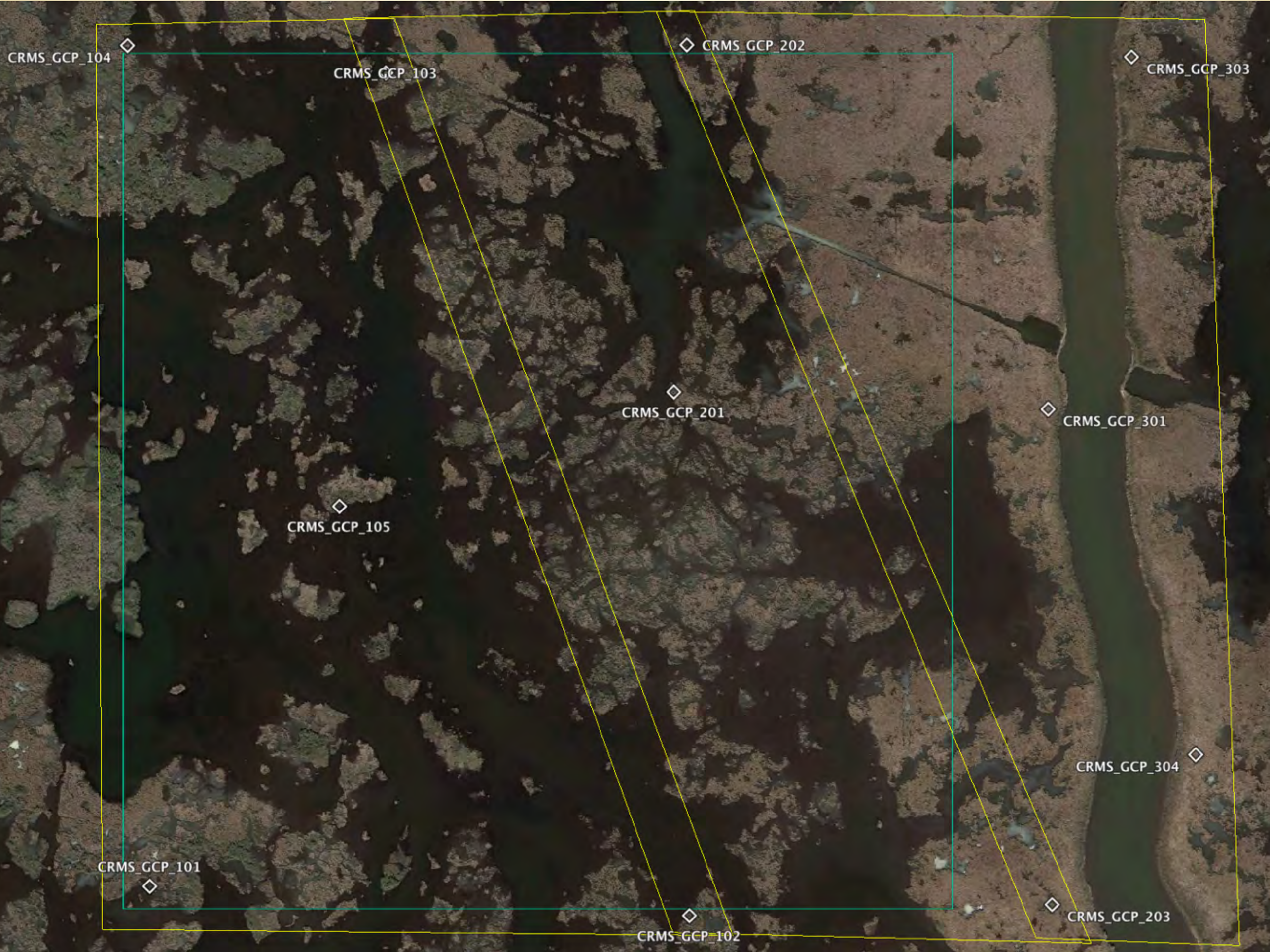
CRMS_GCP_104
CRMS_GCP_103
CRMS_GCP_202
CRMS_GCP_303
CRMS_GCP_201
CRMS_GCP_301
CRMS_GCP_105
CRMS_GCP_304
CRMS_GCP_101
CRMS_GCP_102
CRMS_GCP_203

Ground Control Points

Take Off

Chase home

Control Station

Belly land

Post-Processing: Trimble UAS Master

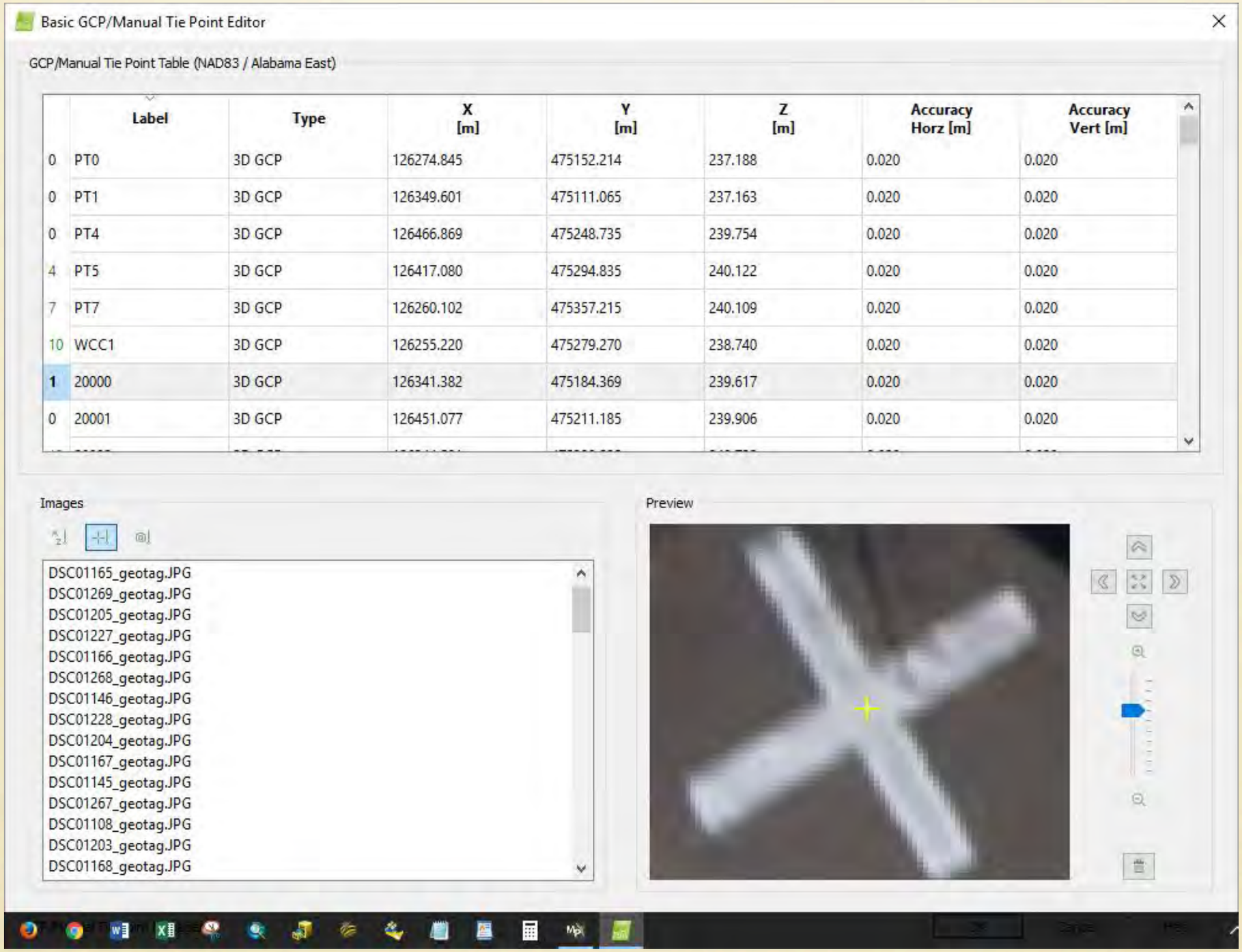

A screenshot of the Basic Editor and the GCP/Manual Tie Point Table showing the location of a ground control point 20000 in image DSC01165_geotag.JPG.

Post-Processing: Trimble UAS Master

Summary

Project	Wiregrass_Broussard
Processed	2016-04-07 23:19:42
Average Ground Sampling Distance (GSD)	1.84 cm / 0.72 in
Area Covered	0.0684 km^2 / 6.8379 ha / 0.0264 sq. mi. / 16.9055 acres
Time for Initial Processing (without report)	11m:07s

Quality Check

Images	median of 33179 keypoints per image	✓
Dataset	89 out of 89 images calibrated (100%), all images enabled	✓
Camera Optimization	1.29% relative difference between initial and optimized internal camera parameters	✓
Matching	median of 14466.8 matches per calibrated image	✓
Georeferencing	yes, 8 GCPs (8 3D), mean RMS error = 0.024 m	✓

A screenshot of the processing quality report showing the summary and quality check information.

	Error X (m)	Error Y (m)	Error Z (m)
Mean (m)	-0.007065	-0.000724	0.015766
Sigma (m)	0.031913	0.018155	0.024366
RMS Error (m)	0.032686	0.018169	0.029022

Localization accuracy per GCP and mean errors in the three coordinate directions.

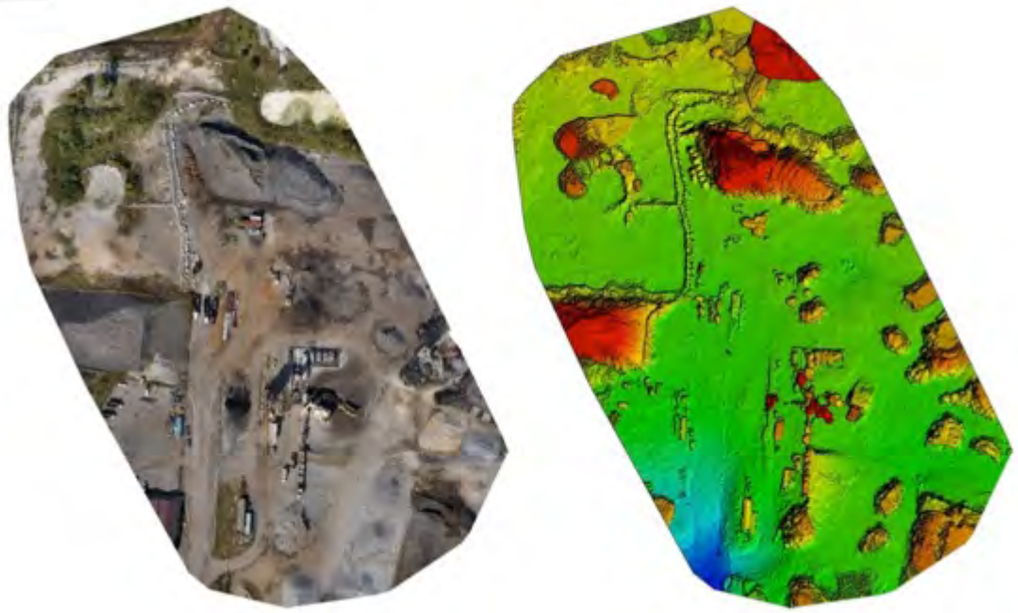

Orthomosaic and the corresponding sparse Digital Surface Model (DSM) before densification

Object Based Image Analysis

i. Hyperspatial sub-decimeter imagery acquired using UAV platforms is commonly analyzed using OBIA classification methods (e.g. Laliberte and Rango 2009, Laliberte and Rango 2011).

ii. For medium and low spatial resolution imagery acquired by satellites, such as Landsat or MODIS, the target is usually smaller than the pixel size. Pixel-based remote sensing classification schemes, like maximum likelihood classifiers that use spectral information, are often unsuitable for classifying hyperspatial data resulting in a lower overall classification accuracy (Blaschke 2010).

iii. As spatial resolution increases, variance in observed spectral values within target classes increases, making spectral separation between the classes more difficult to specify and classify (Marceau and Hay 1999, Blaschke 2010).

iv. OBIA methods address these scaling issues by segmenting the finer pixels into image objects that are made up of multiple neighboring pixels sharing similar spectral values (Blaschke, 2009)

Reference Image

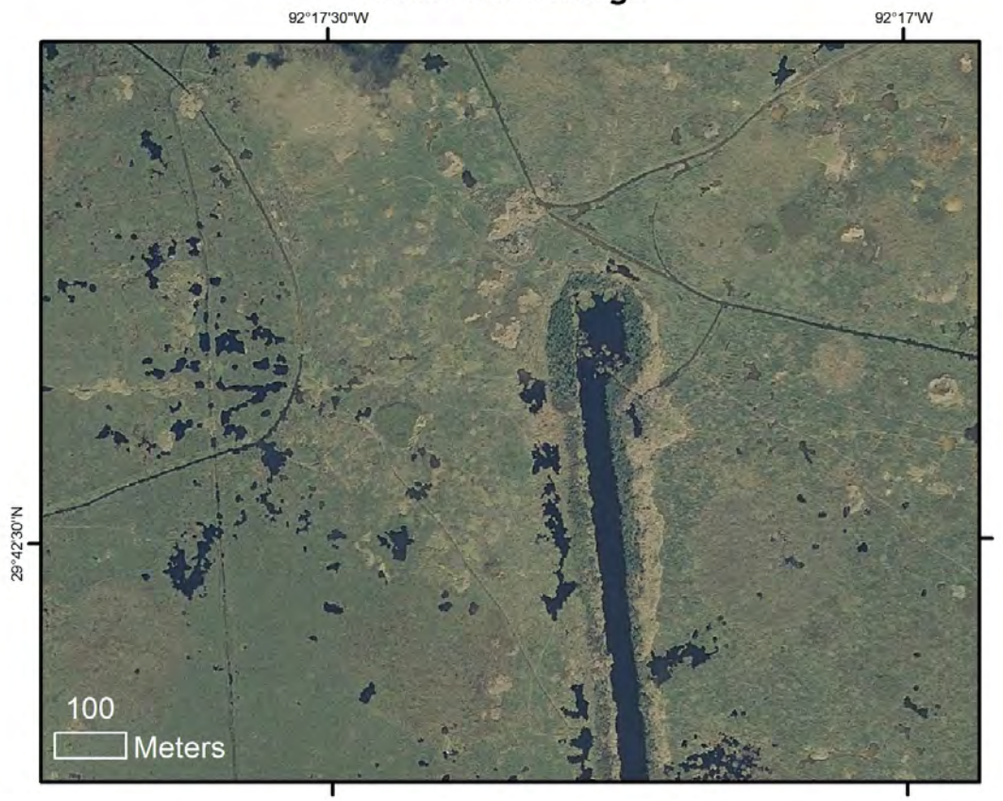

Classified Map

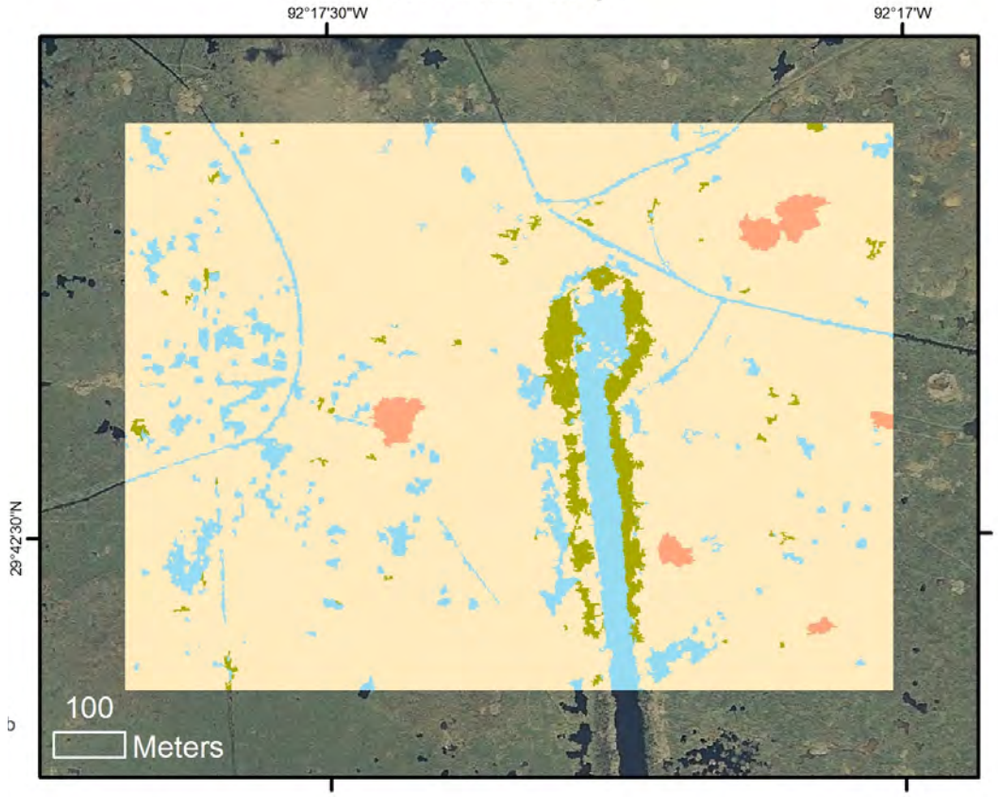

NDVI
- < -1.7 Std. Dev.
- -1.7 - -1.3 Std. Dev.
- -1.3 - -0.75 Std. Dev.
- -0.75 - -0.25 Std. Dev.
- -0.25 - 0.25 Std. Dev.
- 0.25 - 0.75 Std. Dev.
- 0.75 - 1.3 Std. Dev.
- 1.3 - 1.7 Std. Dev.
- 1.7 - 2.2 Std. Dev.
- 2.2 - 2.7 Std. Dev.
- > 2.7 Std. Dev.
- Water

Classification
- Grass
- Reed
- Shrub-Scrub
- Water

NDVI

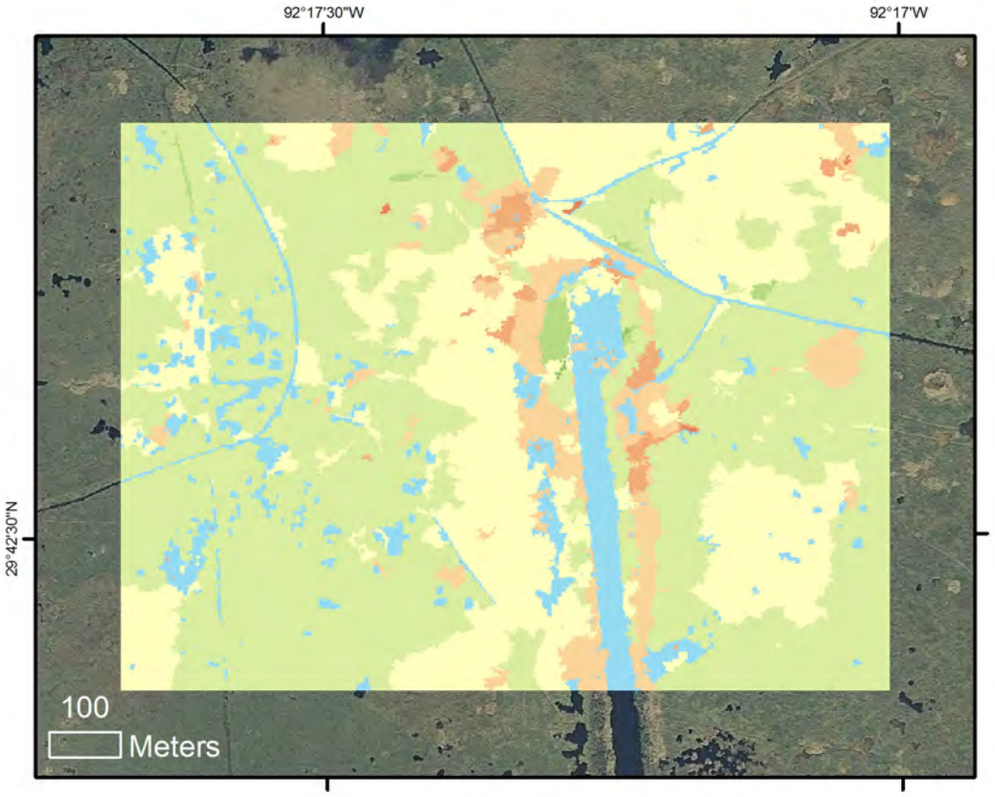

Workflow

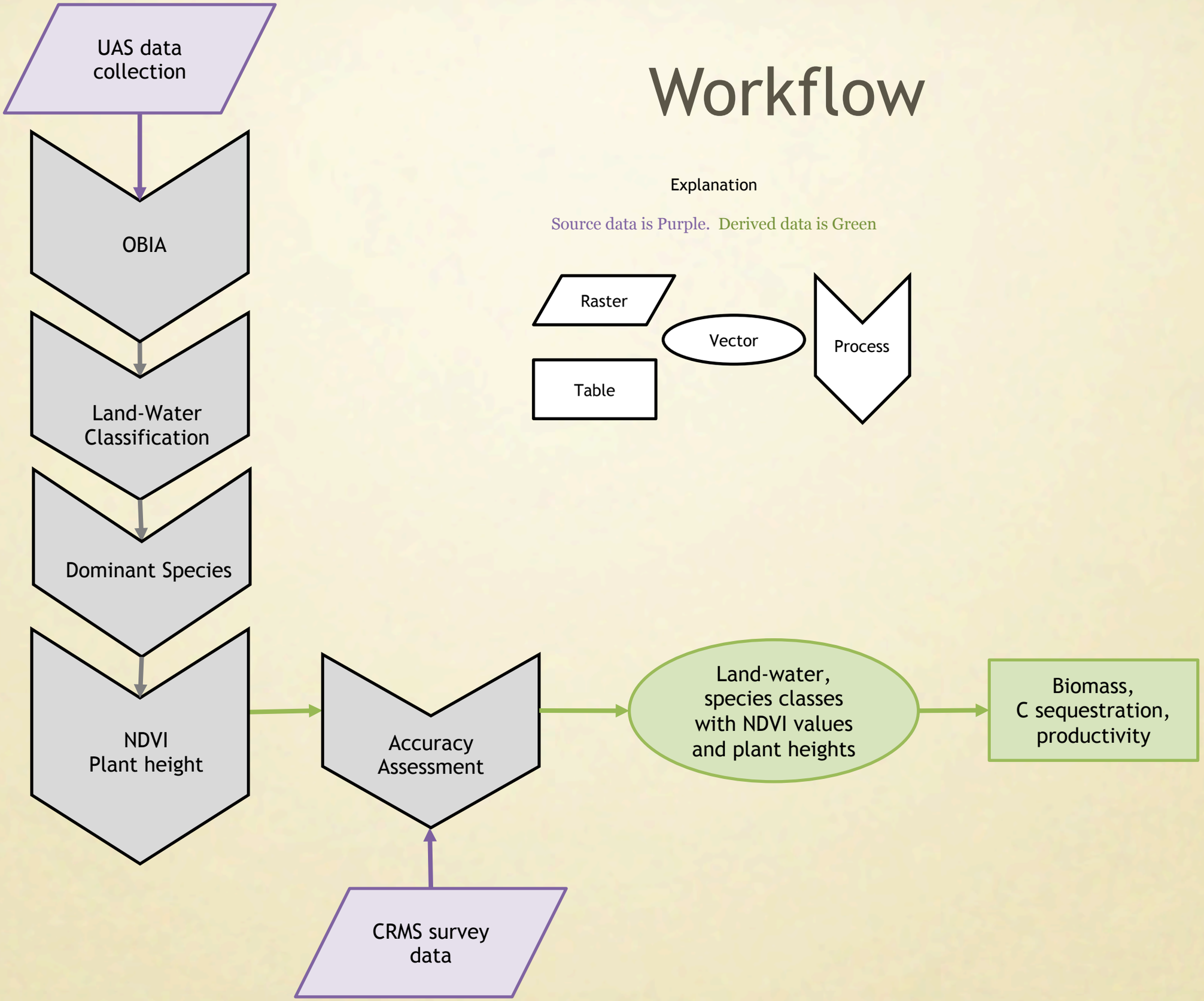

Explanation

Source data is Purple. Derived data is Green

Products and Timeline

i. The purpose of this project is to investigate the efficacy of using UAS technology to monitor wetland vegetation species composition and to quantify ecosystem services. The final deliverable will be a published paper that reports on the methods developed and lessons learned.

ii. Timeline:

- Post-Processing UAS imagery — December-January 2016
- OBIA and Derived Products — January-February 2017
- Draft of Methods and Results — End of February 2017
- Final Report for Publication — March 2017
- Submit for Publication — April 2017

References

Blaschke, T. (2010). Object based image analysis for remote sensing. *ISPRS Journal of Photogrammetry and Remote Sensing*, 65(1), 2–16.

Chong, A.K. (2007) HD aerial video for coastal zone ecological mapping. The 19th Annual Colloquium of the Spatial Information Research Centre.

Chust, G., et al. (2008). Coastal and estuarine habitat mapping, using LIDAR height and intensity and multi-spectral imagery. Estuarine, Coastal and Shelf Science, 78(4), 633–643.

Eisenbeiss, H., Lambers, K., & Sauerbier, M. (2005). Photogrammetric recording of the archaeological site of Pinchango Alto (Palpa, Peru) using a mini helicopter (UAV). Annual Conference on Computer Applications and Quantitative Methods in Archaeology CAA, (March 2005), 21–24.

Klemas, V. (2013). Airborne Remote Sensing of Coastal Features and Processes: An Overview. *Journal of Coastal Research*, 29(2), 239–255.

Klemas, V. (2015). Coastal and Environmental Remote Sensing from Unmanned Aerial Vehicles: An Overview. *Journal of Coastal Research*, 315(5), 1260–1267.

Laliberte, A. S., & Rango, A. (2009). Texture and scale in object-based analysis of subdecimeter resolution unmanned aerial vehicle (UAV) imagery. *IEEE Transactions on Geoscience and Remote Sensing*, *47*(3), 1–10.

Laliberte, A. S., & Rango, A. (2011). Image Processing and Classification Procedures for Analysis of Sub-decimeter Imagery Acquired with an Unmanned Aircraft over Arid Rangelands. *GIScience & Remote Sensing*, 48(1), 4–23.

Laliberte, A. S., et al.. (2011). Multispectral remote sensing from unmanned aircraft: Image processing workflows and applications for rangeland environments. *Remote Sensing*, 3(11), 2529–2551.

Lechner, A. M., et al. (2012). Characterising Upland Swamps Using Object-Based Classification Methods and Hyper-Spatial Resolution Imagery Derived From an Unmanned Aerial Vehicle. ISPRS Annals of Photogrammetry, Remote Sensing and Spatial Information Sciences, I-4(September), 101–106.

Marceau, D., and Hay, G. J (1999). Contributions of remote sensing to the scale issue. *Canadian Journal of Remote Sensing*, 25(4), 357–366.

Niethammer, U., et al. (2012). UAV-based remote sensing of the Super-Sauze landslide: Evaluation and results. Engineering Geology, 128, 2–11.

Phinn, S. R., et al. (1996). Monitoring Wetland Habitat Restoration in Southern California Using Airborne Multi spectral Video Data. *Restoration Ecology*, 4(4), 412–422.

Przybilla, H.-J., & Wester-Ebbinghaus, W. (1979). Bildflug mit ferngelenktem Kleinflug- zeug. Bildmessung Und Luftbildwesen Zeitschrift Fuer Photogrammetrie Ferner- Kundung, 47(5), 137–142.

Rocchini, D. (2007). Effects of spatial and spectral resolution in estimating ecosystem diversity by satellite imagery. *Remote Sensing of Environment*, 111(4), 423–434.

Yang J., Artigas F. J., (2010) Mapping salt marsh vegetation by integrating hyperspectral and LiDAR remote sensing. In: Wang, J. (ed.). Remote Sensing of Coastal Environments. Boca Raton, FL: CRC, pp. 173–190.

THANK YOU!

Whitney Broussard
wbroussardiii@gmail.com